Journal of Alloys and Compounds 769 (2018) 843–847

Contents lists available at ScienceDirect

Journal of Alloys and Compounds

journal homepage: http://www.elsevier.com/locate/jalcom

# Structural and magnetic properties of hexagonal $Fe_3Sn$ prepared by non-equilibrium techniques

C. Echevarria-Bonet [a, *], N. Iglesias [a, b], J.S. Garitaonandia [a, b], D. Salazar [a], G.C. Hadjipanayis [c], J.M. Barandiaran [a, b]

[a] BCMaterials, Basque Centre for Materials, Applications and Nanostructures, UPV/EHU Science Park, 48940 Leioa, Spain
[b] Faculty of Science & Technology, University of the Basque Country (UPV/EHU), Leioa, Spain
[c] Department of Physics and Astronomy, University of Delaware, Newark DE, USA

ARTICLE INFO

*Article history:*
Received 1 August 2017
Received in revised form
30 June 2018
Accepted 23 July 2018
Available online 29 July 2018

*Keywords:*
Permanent magnets
Solid state reactions
Mechanical alloying
Magnetic measurements
XRD
Mössbauer spectroscopy

ABSTRACT

We report a thorough structural and magnetic study of $Fe_3Sn$ produced either by solid state reaction or by mechanical alloying in order to figure out which of the two techniques is most suitable for obtaining the purest $Fe_3Sn$ alloy. Solid state reaction of Fe and Sn starting powders results in a pure sample (100%) of $Fe_3Sn$. The extraordinary purity and crystallinity have been confirmed by in-lab XRD and Mössbauer spectroscopy. This study has been completed by magnetic measurements M(H) and M(T); a saturation magnetization of 122 A $m^2$/kg and Curie temperature $T_c = 475\,^{\circ}C$, have been obtained.



## 1. Introduction

During the last century, the intense research on hard magnetic materials led to a continuous increase of permanent magnets (PM) development. The current PM markets consists mostly of inexpensive ferrites with moderate performance used in small motors or electronic components to high performance and expensive rare-earth (RE) magnets like $Nd_2Fe_{14}B$ and $SmCo_5$ used in large motors, generators and magnetic resonance imaging equipment among others.

The stored energy of a PM is given by its energy product (BH) (B the induction), so that a large (BH) value is desirable in working conditions. In fact, the maximum energy product $(BH)_{max}$ that a PM can provide is its figure of merit. Other important properties that define a PM are the remanence $M_r$, coercivity $H_C$ (related to the anisotropy field $H_a$) and Curie temperature $T_C$. A high value of $T_C$ is mandatory in order to have a wide T-range for applications.

PMs experienced a tremendous development during the 20th century and their performance increased 5-fold only from 1960 (with Alnico systems) to 1985 (with the discovery and development of Nd-Fe-B magnets). However, in the last decades no further improvements have been found in the figure of merit, which reached the maximum value of 56 MGOe in Nd-Fe-B. The key of the good performance of RE-containing PM is the good balance between the high magnetocrystalline anisotropy provided by the large spin-orbit coupling of the 4f-elements (RE elements) and the large saturation magnetization given by the transition metal element (mostly Fe). As a result, high performance permanent magnets are totally dependent on scarce and expensive RE elements such as Dy, Nd or Tb, which are now considered as critical raw materials (CRM), and China is the main producer and exporter (97% of global supply). Lately, a global increasing demand has been registered as RE elements are used in electronic components such as mobile phones, displays and, as commented above, in permanent magnets, amongst others, while the Chinese export quota is steady since 2010 and decreased at least two-fold in the previous years [1]. This worrying situation makes the development of RE-free PM an urgent priority and presents a great scientific and technological challenge. In this sense, the European Comission [2] and the Department of Energy (USA) [3] wrote policies in order to develop RE-lean and RE-free PM. Advances and current research in RE-free PM can be found

* Corresponding author.
*E-mail address:* echevarria.cristina@gmail.com (C. Echevarria-Bonet).

https://doi.org/10.1016/j.jallcom.2018.07.257

in Refs. [4–7]. Our motivation in this work is to develop a RE-free material.

One material to be considered for PM applications is $Fe_3Sn$. However, although it has a hexagonal structure and large magnetization, it presents planar anisotropy, not suitable for PM applications. This compound has absolutely no RE elements and its constituents are inexpensive and abundant. However, the hexagonal phase of $Fe_3Sn$ (spatial group $P6_3/mmc$) is only stable in the temperature range 750–880 °C, as indicated in the Fe-Sn equilibrium phase diagram [8]. Thus, this metastable phase cannot be achieved by standard methods, such as arc or induction melting. Instead, it has been reported that it can be obtained by solid state reaction (SSR) [9,10] or mechanical alloying (MA) [8,9], though in the latter case, a non-negligible percentage of bcc-Fe was still present after the best processing, as shown by Mössbauer spectroscopy [11]. Other works reported that both Fe and Sn Mössbauer spectra of $Fe_3Sn$ consist in single sextets [11,13]. Trumpy et al. (1970) [13] claims that the existence of a single sextet proves that the magnetization is directed along the c-axis. However, direct magnetic measurements indicate the existence of planar anisotropy for the $Fe_3Sn$ alloy [9]. There is a certain controversy on the nature of the $Fe_3Sn$ anisotropy. In any case, there are very few reports on the magnetic properties of $Fe_3Sn$ [13,14], in contrast with the possible interest of such alloy for PM.

In this work, we report a thorough structural and magnetic study of $Fe_3Sn$ produced either by solid state reaction or by mechanical alloying, in order to fill out this gap and to figure out which of the two techniques is most suitable for obtaining the purest $Fe_3Sn$ alloy.

## 2. Material and methods

$Fe_3Sn$ alloys were prepared by either solid state reaction (SSR) or mechanical alloying followed by heat treatment (MA+HT), through the following procedures. In the first case, stoichiometric amounts of powders of the starting elements (99.9+% purity, particles of less than 50 μm in size) were hand-milled in an agate mortar and pestle and then compacted into pellets using pressures up to 0.5 GPa at room temperature (RT). Pellets were encapsulated in a quartz ampoule, heated to 800 °C for 48 h in vacuum and then quenched into ice water. This procedure was repeated twice in order to achieve a full reaction and homogenize the composition of the samples. For MA, Fe and Sn powders were sealed, under Argon atmosphere, in hardened steel vials with a ball-to-powder ratio of 10:1, and then milled for 24 h, in a SPEX 8000D mill. The resulting powders were heat-treated at different temperatures for 18 and 48 h in Argon atmosphere and then quenched in ice water. The difference between the two methods lies on the starting nature of the processed powders. For SSR, we are using pure and Fe and Sn and for MA the powders consist of an amorphous solid solution of Fe and Sn.

X-Ray Diffraction (XRD) was carried out on a Philips X'Pert Pro diffractometer, in the Bragg-Brentano geometry, using Cu K$\alpha$ radiation ($\lambda = 1.5418$ Å). The samples were placed on a spinner to limit preferential crystalline orientation. XRD patterns were analyzed by Rietveld refinements, through the FullProf Suite [15], using a Thompson-Cox-Hastings pseudo-Voigt function to describe the profile of the peaks. Direct determination of the composition of the samples was done by EDS in a scanning electron microscope (SEM, JEOL JSM-6400).

$^{57}$Fe and $^{119}$Sn Mössbauer spectra were acquired at RT using a conventional constant-acceleration spectrometer in standard transmission geometry with $^{57}$Co-Rh and a $Ba^{119}SnO_3$ sources, respectively. The NORMOS (1990) software package developed by R. Brand [16] was used to fit these spectra.

Magnetic measurements, at room temperature and above, were carried out in a vibrating sample magnetometer EZ7-VSM from Microsense, in magnetic fields up to 1.85 T.

## 3. Results and discussion

### 3.1. Synthesis of the alloys and structural characterization

#### 3.1.1. Solid state reaction

XRD patterns and SEM pictures (with elemental mappings) of $Fe_3Sn$, are shown in Fig. 1, after one (1SSR) and two (2SSR) solid state reactions. The inset of Fig. 1(a) (1SSR) shows a clear segregation of Fe and Sn. For 2SSR, however, the alloying of Fe and Sn is complete, as seen in the inset of Fig. 1(b). This is confirmed by the Rietveld refinement of the XRD patterns, which gives 78.8 wt% of $Fe_3Sn$, 13.2 wt% of bcc-Fe, and 8.0 wt% of $Fe_3Sn_2$ for 1SSR, while for 2SSR is 100% of $Fe_3Sn$. This is in very good agreement with SEM-EDS results. We, therefore, conclude that there is a need to repeat the SSR at least twice to obtain the pure $Fe_3Sn$ phase.

The Rietveld refinement of the XRD of a powder polycrystalline sample of 2SSR-$Fe_3Sn$ is shown in Fig. 1(b) and the crystal structure

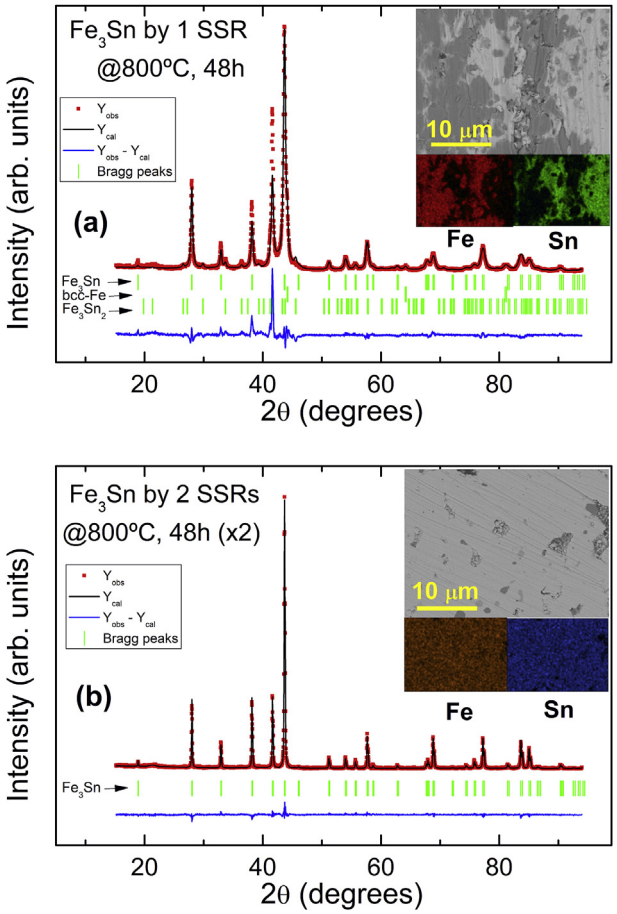


**Fig. 1.** **(a)** Rietveld refinement of the XRD pattern of the $Fe_3Sn$ sample, produced by 1 SSR (at 800 °C for 48 h). Several phases are present: $Fe_3Sn$, bcc-Fe and $Fe_3Sn_2$. SEM photograph of the sample, where a segregation of Fe and Sn is clearly visible, confirmed by the SEM-EDS elemental mapping images for Fe (red) and Sn (green). **(b)** Rietveld refinement of the XRD pattern of the $Fe_3Sn$ sample, produced by 2 subsequent SSRs (at 800 °C for 48 h). Only one phase is present in this pattern, hexagonal $Fe_3Sn$. SEM photograph of the sample shows the complete alloying of Fe and Sn, confirmed by the SEM-EDS elemental mapping images for Fe (orange) and Sn (blue). (For interpretation of the references to colour in this figure legend, the reader is referred to the Web version of this article.)

can be described as the hexagonal $Ni_3Sn$ structure (space group $P6_3/mmc$), with lattice parameters a = 5.4620(1) Å and c = 4.3490(1) Å, where Fe and Sn atoms are located in the 6 h (0.849, 0.698, 0.25) and 2c (0.333, 0.667, 0.25) sites. A slight deficiency in Sn element is also obtained from the Rietveld refinement, as occupancies of 0.02505 and 0.0826 are obtained. If we normalize these values, the Fe and Sn-site occupancies are 0.25 and 0.0824, as compared to the theoretical 0.25 and 0.0833, respectively. Thus, there could be some extra Fe atoms (or Sn vacancies) along the sample that cannot be observed by XRD. EDS confirms that the stoichiometry of the sample, $Fe_{76.5(1.8)}Sn_{23.5(1.2)}$, is slightly Sn defective.

### 3.1.2. Mechanical alloying

Mechanical alloying was performed as described above. The as-milled alloy (black line) consists of a disordered Fe-Sn bcc-solid solution, characterized by broad peaks in the XRD pattern (see Fig. 2), with lattice parameter a = 2.993(2) Å. Differential Scanning Calorimetry (DSC) (see inset of Fig. 2) shows a crystallization temperature $T_{crys}$ = 365 °C, in good agreement with a thermodiffractogram also performed on the milled alloy (not shown in here).

Thus, several heat treatments were chosen for processing the as-milled alloys to the desired hexagonal $Fe_3Sn$ structure: $T_1$ = 400 °C, from the DSC results, $T_2$ = 600 °C as a previous work [11] reported obtaining the $Fe_3Sn$ phase after a crystallization process at 550 °C for 5 h and, finally, $T_3$ = 800 °C, due to the stability region of $Fe_3Sn$ in the Fe-Sn phase diagram [8] and the previous results by SSR. We used 18 h treatment for every temperature.

XRD of the resulting samples are shown in Fig. 2. For samples crystallized at 400 and 600 °C (red and green lines, respectively), a phase other than $Fe_3Sn$ is observed. Actually, the patterns correspond to a mixture of FeSn and bcc-Fe(Sn). In the sample crystallized at 400 °C, there is still a clear contribution from the disordered Fe-Sn bcc-solid solution. These results are in contrast with those from Ref. [11], were they claimed the procuration of the $Fe_3Sn$ phase after only 5 h at 550 °C.

In our case, only the sample crystallized at 800 °C (for 18 h, blue line) consists of a major contribution of $Fe_3Sn$ and a small content of bcc-Fe rich phase (hereinafter, MA+HT800 °C_18 h). A longer crystallization process (48 h, purple line) was thus performed in order to reduce this secondary phase (hereinafter, MA+HT800 °C_48 h). From the Rietveld refinements (see Table 1), a reduction of the bcc-Fe phase, from 10.3 wt% in 18 h treatment to 7.2 wt% in 48 h is observed. The lattice parameters of the 3:1 phase for the MA+HT800 °C_18 h and MA+HT800 °C_48 h samples are a = 5.4658(1) Å and c = 4.3530(1) Å and a = 5.4637(1) Å and c = 4.3512(1) Å, respectively. These are very similar to those of the SSR sample. The lattice parameter for the bcc-Fe rich phases are a = 2.9149(1) Å and a = 2.9119(1) Å for MA+HT800 °C_18 h and MA+HT800 °C_48 h, respectively. Following Vegard's rule, as published in Ref. [8], these lattice parameters correspond to a solid solution of Sn in Fe, with compositions around $Fe_{93.8}Sn_{6.2}$ and $Fe_{93.4}Sn_{6.6}$, very similar to each other. Therefore, we can assume that, for longer treatments, there is no further reaction between Fe and Sn to produce a different bcc-Fe(Sn) phase, but only a partial recombination of the bcc phase with the $Fe_3Sn$ one, to increase the amount and produce a slight compositional change.

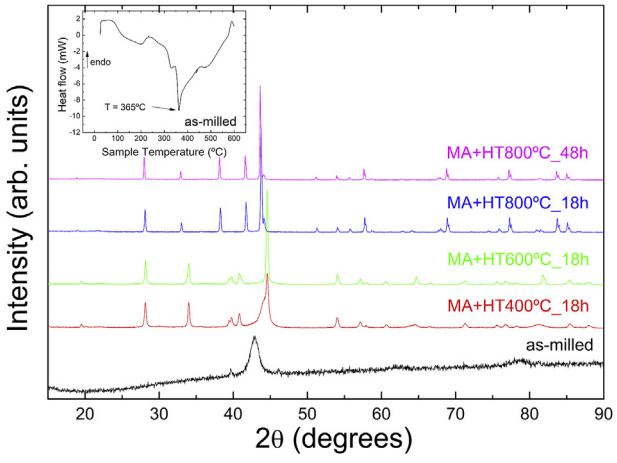


**Fig. 2.** XRD patterns of the as-milled (black) $Fe_3Sn$ alloy and its subsequent heat treatments at 400 °C (red), 600 °C (green) and 800 °C for 18 h (blue) and at 800 °C for 48 h (purple). Inset: Differential Scanning Calorimetry of the as milled sample, with a characteristic crystallization temperature of 365 °C. (For interpretation of the references to colour in this figure legend, the reader is referred to the Web version of this article.)

We can expect than even longer heat treatments would eventually lead to the pure $Fe_3Sn$ phase. However, as we are looking for the most efficient technique to obtain the $Fe_3Sn$ phase, we can conclude that Solid State Reaction is much better than Mechanical Alloying and Heat Treatment.

### 3.2. Local magnetic properties

In Fig. 4, the fitted $^{57}$Fe (left) and $^{119}$Sn (right) Mössbauer spectra of the $Fe_3Sn$ the sample produced by both SSR and MA (with a subsequent heat treatment at 800 °C, for 48 h, i.e. the MA+HT800 °C_48 h sample) are shown. Values of the hyperfine parameters of the spectra obtained after the fitting are shown in Table 2.

$^{57}$Fe Mössbauer spectra of both SSR and MA $Fe_3Sn$ samples show a well resolved sextet, around 4 mm/s, with same hyperfine parameters. This component emanates from the $Fe_3Sn$ phase [14] and describes a crystalline phase with a single non-equivalent Fe site in agreement with the crystallographic structure deduced from the refinement of the XRD. $^{57}$Fe Mossbauer spectrum of MA $Fe_3Sn$ sample also shows two additional components associated to a bcc-Fe(Sn) solid solution phase, and related to Fe sites with 8 Fe atoms and 7 Fe and 1 Sn atoms in its respective neighborhoods (labeled as *bcc-FeSn 0 Sn nn* and *bcc-FeSn 1Sn nn* on Table 2 and Fig. 3). The relative Fe quantities of these two components are 7.1 and 4.2 at.%, respectively, which perfectly fits with the relative probabilities expected from a binomial distribution of a bcc-Fe(Sn) solid solution alloy with a composition as deducted from the refinement of the XRD. Therefore, the relative Fe quantity for the bcc-Fe(Sn) rises up to 11.3 at.%, also in a good agreement with the 7.2 wt% estimated from XRD for this phase. No trace of bcc-Fe is observed in the $^{57}$Fe Mössbauer spectrum of the 2SSR-$Fe_3Sn$ sample.

With regard to the $^{119}$Sn Mössbauer spectra, both samples give rise to non-totally resolved spectra. These spectra can be properly fitted by an only sextet with similar hyperfine parameters, which would indicate that the $Fe_3Sn$ phase has been generated without excess of Sn. In the spectrum corresponding to the MA $Fe_3Sn$ sample it would be expected a contribution from the bcc-Fe(Sn) phase. However, from the XRD and $^{57}$Fe Mössbauer results it has been estimated that only 2–3% of the total Sn atoms are located in this phase. Its $^{119}$Sn Mossbauer spectral component would be obscured in the background so that it has not been taken into account.

On the other hand, it has been observed that both $^{57}$Fe and $^{119}$Sn Mössbauer spectra of the SSR sample are broader that those corresponding to the MA $Fe_3Sn$ sample. The width of a spectrum is normally associated to the atomic ordering around the Mössbauer nuclei. Therefore, from Mössbauer spectroscopy, it can be concluded that $Fe_3Sn$ phase obtained from crystallization of the

**Table 1**
Lattice parameters a, c and percentages for the $Fe_3Sn$ and bcc-Fe phases, with the RB error, as calculated from Rietveld refinements of the XRD data, for the $Fe_3Sn$ produced by the different methods.

| Synthesis method | $Fe_3Sn$ | | | | bcc-Fe | | |
|---|---|---|---|---|---|---|---|
| | a (Å) | c (Å) | % | $R_B$ (%) | a (Å) | % | $R_B$ (%) |
| 1 SSR | 5.4618(3) | 4.3527(3) | 78.8(1.3) | 14.9 | 2.9082(3) | 13.2(6) | 6.0 |
| 2 SSR | 5.4620(1) | 4.3490(1) | 100.0(1.2) | 5.6 | – | 0 | – |
| MA+HT800 °C_18 h | 5.4658(1) | 4.3530(1) | 89.7(7) | 9.2 | 2.9149(1) | 10.3(3) | 9.4 |
| MA+HT800 °C_48 h | 5.4637(1) | 4.3512(1) | 92.8(7) | 6.7 | 2.9119(1) | 7.2(2) | 20.0 |

**Table 2**
Values of IS isomer shift, QS quadrupole shift, $B_{hf}$ hyperfine field and Γ line-width obtained from the fitting of the Mössbauer spectra for the studied samples. Isomer shifts values were referred to bcc-Fe at 295 K. *The % Fe refers to the Fe in each phase out of the total Fe in the sample.

| Sample (phase) | $^{57}$Fe source | | | | $^{119}$Sn source | | | | % Fe |
|---|---|---|---|---|---|---|---|---|---|
| | IS (mm/s) | QS (mm/s) | $B_{hf}$ (T) | Γ (mm/s) | IS (mm/s) | QS (mm/s) | $B_{hf}$ (T) | Γ (mm/s) | |
| 2SSR ($Fe_3Sn$) | 0.30(1) | 0.15(1) | 25.0(1) | 0.37(1) | 1.56(1) | 0.09(1) | 7.8(1) | 1.61(1) | 100 |
| MA+HT800 °C_48 h ($Fe_3Sn$) | 0.30(1) | 0.14(1) | 25.1(1) | 0.34(1) | 1.50(1) | 0.03(1) | 7.8(1) | 1.25(1) | 87.4 |
| MA+HT800 °C_48 h (Bcc-FeSn 0Sn nn) | 0.0(1) | 0.00(1) | 33.3(2) | 0.33(1) | – | – | – | – | 7.1 |
| MA+HT800 °C_48 h (Bcc-FeSn 1Sn nn) | 0.12(1) | 0.00(1) | 31.4(1) | 0.33(1) | – | – | – | – | 4.2 |

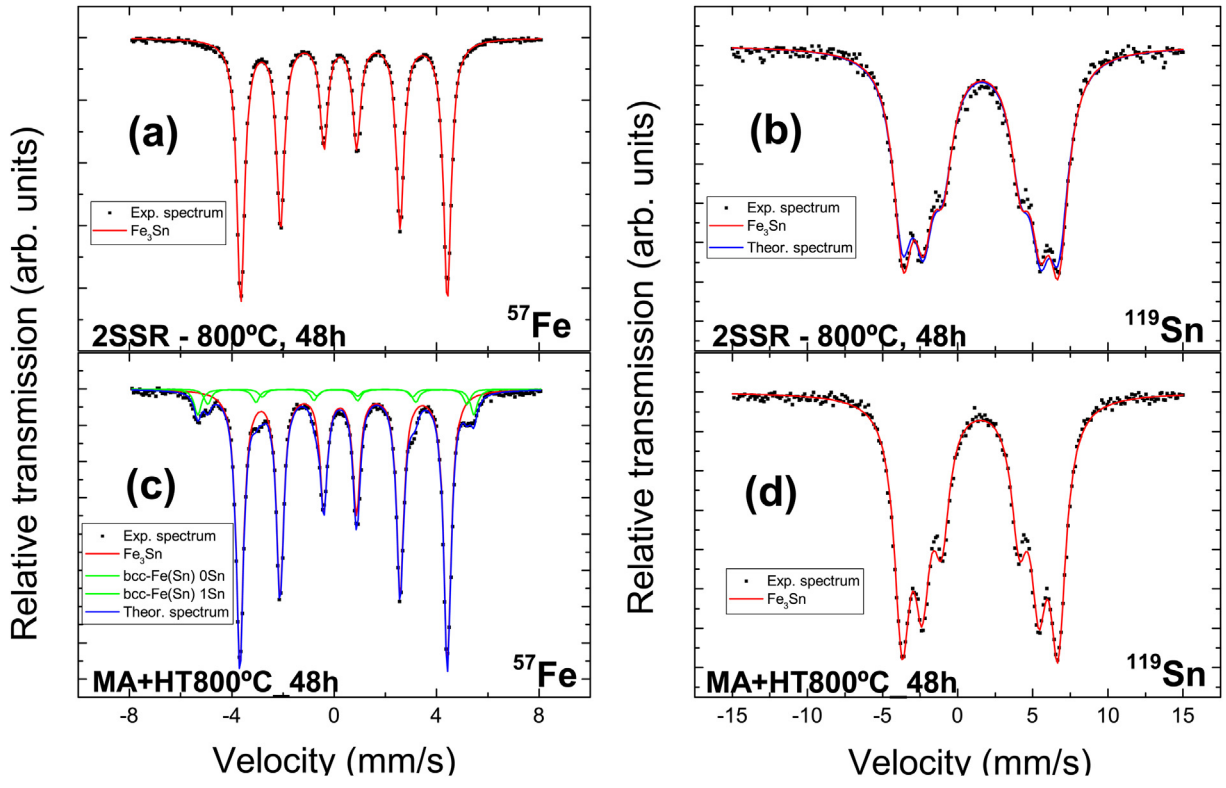


**Fig. 3.** Mössbauer spectra obtained for the 2SSR-$Fe_3Sn$ ($Fe_3Sn$ produced by 2 SSRs) absorber at room temperature, using **(a)** $^{57}$Fe and **(b)** $^{119}$Sn sources, and for the MA+HT800 °C_48 h-$Fe_3Sn$ ($Fe_3Sn$ produced by mechanical alloying and heat treated at 800 °C for 48 h), using **(c)** $^{57}$Fe and **(d)** $^{119}$Sn sources. In the case of 2SSR-$Fe_3Sn$, only a contribution from the $Fe_3Sn$ phase can be observed, with no sign of bcc-Fe, as in other works [8]. However, for the mechanically alloyed $Fe_3Sn$, apart from the $Fe_3Sn$, a remaining contribution from bcc-Fe is visible in (c). We can conclude that it is not a bcc-(Fe,Sn) solid solution as no contribution from a second phase is present in (d).

mechanically alloyed sample presents a higher degree of crystallinity, even if residual Fe quantities are also observed.

### 3.3. Macroscopic magnetic properties

To study the nature of the magnetocrystalline anisotropy of $Fe_3Sn$, fine powders were embedded in an epoxy and oriented with a magnetic field of H = 1.85 T while curing takes place. The hysteresis loops of the field-oriented powders are shown in Fig. 4 (center) for the parallel (blue closed symbols) and perpendicular (red open symbols) directions with respect to the applied magnetic field. They are characteristic of a planar magnetic anisotropy, i.e., the easy direction of the magnetization lies in the basal plane of the hexagonal structure. Our measurements confirm a previous work from B.C. Sales et al. [6] but opposes to Trumpy et al. [13], who claimed that the easy magnetic axis is the c-axis, from an indirect analysis of Mössbauer measurements. In the left inset we extrapolate the parallel and perpendicular magnetization curves to

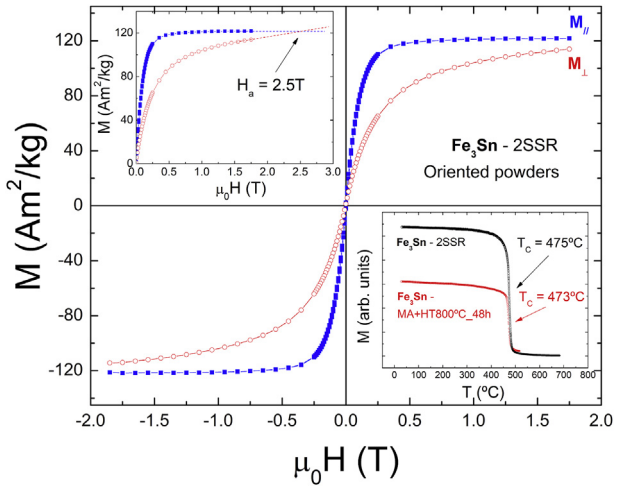


**Fig. 4.** Parallel (blue) and perpendicular (red) M(H) curves for the field-oriented powders of the $Fe_3Sn$-2SSR sample. Inset **(a)** represents the extrapolation of the parallel and perpendicular magnetization curves in order to obtain an approximate value of the anisotropy field $H_a$ where these merge, $\mu_0 H_a = 2.5$ T. Inset **(b)**: Temperature dependent magnetization for 2SSR-$Fe_3Sn$ and MA+HT800 °C_48 h-$Fe_3Sn$, using a magnetic field of 0.01 T. The Curie temperatures have been determined by the first derivative of the magnetization to be approximately 475 °C for 2SSR-$Fe_3Sn$ and 473 °C for the MA+HT800°C_48 h-$Fe_3Sn$ samples. (For interpretation of the references to colour in this figure legend, the reader is referred to the Web version of this article.)

determine the anisotropy field $H_a$, obtaining a value of $\mu_0 H_a = 2.5$ T. Using the well-known approximation:

$$K_1 \approx \frac{H_a M_S}{2}$$

where $M_S$ is the saturation magnetization ($M_S = 122$ A m$^2$/kg), we can obtain an approximated value for the first anisotropy constant: $K_1 = 1.29$ MJ/m$^3$. This value is somewhat lower than the experimental one obtained by B. C. Sales et al. ($K_1 = 1.8$ MJ/m$^3$) [9] but closer to the theoretically ones predicted by B. C. Sales et al. ($K_1 = 1.59$ MJ/m$^3$) [9] and P. Nieves et al. ($K_1 = 1.47$ MJ/m$^3$) [17].

The temperature dependence of the magnetization of the SSR sample, using a magnetic field $\mu_0 H = 0.01$ T, is shown in Fig. 4 (right) and a Curie temperature $T_C = 475$ °C has been determined through the first derivative of the magnetization, $\partial M/\partial T$, a very similar value to those reported in literature [18]. For the mechanically alloyed and heat treated sample (MA 800 °C, 48 h), the Curie temperature was 473 °C, very similar to the SSR sample.

## 4. Conclusions

The hexagonal $Fe_3Sn$ phase has been produced by two different methods: solid state reaction and mechanical alloying. Solid state reaction is the most suitable method to obtain the pure $Fe_3Sn$ phase. XRD, SEM and Mössbauer spectroscopy confirm the extraordinary purity of the alloy. Mechanical alloying and thermal treatments up to 48 h at 800 °C still shows a 7% bcc-Fe rich phase present. Magnetic measurements show that the pure phase has planar magnetic anisotropy, as previously reported in the literature, with a first constant ($K_1$) value close to the theoretical predictions.

## Acknowledgements

Authors acknowledge support from NOVAMAG project, under Grant Agreement No. 686056, EU Horizon 2020 Framework Programme for Research and Innovation (2014–2020).

## References

[1] S. Massari, M. Ruberti, Resour. Pol. 38 (2013) 36–43.
[2] European Commission, Critical Raw Materials for the EU. Report of the Ad-hoc Working Group on Defining Critical Raw Materials, European Commission, Enterprise and Industry, 2010. June.
[3] US DOE, Critical Material Strategy, 2010. December 2010.
[4] R.W. McCallum, L.H. Lewis, R. Skomski, M.J. Kramer, I.E. Anderson, Annu. Rev. Mater. Res. 44 (2014) 451–477.
[5] N. Poudyal, J.P. Liu, J. Phys. D Appl. Phys. 46 (2013), 043001.
[6] E. Lottini, et al., Chem. Mater. 28 (12) (2016) 4214–4222.
[7] L.H. Lewis, F. Jimenez Villacorta, Metall. Mater. Trans. A 44 (2012) 2–20.
[8] B. Predel, Fe-sn (Iron-tin), Springer Berlin Heidelberg, Berlin, 1995. O. K. von Goldbeck, Iron-Tin Fe-Sn, Springer Berlin Heidelberg, Berlin, 1982.
[9] B.C. Sales, B. Saparov, M.A. McGuire, D.J. Singh, D.S. Parker, Sci. Rep. 4 (2014) 7024.
[10] H. Giefers, M. Nicol, J. Alloys Compd. 422 (12) (2006) 132–144.
[11] C. Bansal, Z.Q. Gao, L.B. Hong, B. Fultz, J. Appl. Phys. 76 (10) (1994) 5961–5966.
[13] G. Trumpy, E. Both, C. Djéga-Mariadassou, P. Lecocq, Phys. Rev. B 2 (1970) 3477–3490.
[14] C. Djéga-Mariadassou, P. Lecocq, G. Trumpy, J. Träff, P. Østergaard, Nuovo Ciment. B (1965-1970) 46 (1) (1966) 35–45.
[15] J. Rodríguez-Carvajal, Physica B 192 (1993) 55–69.
[16] R.A. Brand, Normos Mössbauer Fitting Program, Univ. Duisburg, 2002.
[17] P. Nieves, S. Arapan, G.C. Hadjipanayis, D. Niarchos, J.M. Barandiaran, S. Cuesta-López, Phys. Status Solidi (c) 13 (2016) 942–950.
[18] C. Jannin, A. Michel, P. Lecocq, Cr. Hebd. Acad. Sci. 257 (1963) 1906–1907.